The Influence of Production and Destruction of O Isotopes in Red Giant Stars

Ahmed Abdul-Razzaq Selman
Department of Astronomy and Space, College of Science, University of Baghdad

Abstract

Thermonuclear reaction rates are calculated for three oxygen isotopes ^{14,15,16}O in CNO cycles reactions occurring in red giant stars. These reactions are: $^{19}\text{F}(p,\alpha)^{16}\text{O}$, $^{15}\text{N}(p,\gamma)^{16}\text{O}$, $^{14}\text{N}(p,\gamma)^{15}\text{O}$, $^{18}\text{F}(p,\alpha)^{15}\text{O}$, $^{13}\text{N}(p,\gamma)^{14}\text{O}$, $^{15}\text{O}(\alpha,\gamma)^{19}\text{Ne}$ and $^{16}\text{O}(p,\gamma)^{17}\text{F}$. Reaction rates have been calculated using MATLAB codes, and related comparisons were made with NACRE II and Reaclib libraries, and the ratios of production to the destruction of ^{15,16}O isotopes were found. Present reaction rate results were close to most of the selected reactions, and in some cases larger with a factor of 1-3. ^{15,16}O production to destruction ratios indicated a special tendency to saturate at temperatures higher than ~ 2 GK, and these ratios were in general larger than 1 indicating an excess of producing such isotopes in red giant stars.

Keywords: Nucleosynthesis, Astrophysics, Nuclear Physics, CNO Cycle, Reaction Rates, Stellar Physics

<div dir="rtl">

تأثير انتاج وتدمير نظائر الاوكسجين في النجوم العمالقة الحمر

أحمد عبد الرزاق سلمان

قسم الفلك والفضاء ، كلية العلوم ، جامعة بغداد، بغداد، العراق

الخلاصة

تم حساب التفاعلات النووية لثلاث من نظائر الأوكسجين ^{14,15,16}O اثناء دورة كربون–نتروجين–اوكسجين في النجوم العمالقة الحمر. هذه التفاعلات هي ، $^{19}\text{F}(p,\alpha)^{16}\text{O}$, $^{15}\text{N}(p,\gamma)^{16}\text{O}$, $^{14}\text{N}(p,\gamma)^{15}\text{O}$, $^{18}\text{F}(p,\alpha)^{15}\text{O}$, $^{13}\text{N}(p,\gamma)^{14}\text{O}$, $^{15}\text{O}(\alpha,\gamma)^{19}\text{Ne}$. تم احتساب معدلات التفاعل النووي للتفاعلات أعلاه وذلك بكتابة عدة برامج بلغة ماتلاب ومقارنة النتائج مع المكتبات العالمية (ناكري 2) و (رياكلب). ثم أجريت حسابات لتقدير انتاج الى استهلاك نظائر الاوكسجين 15 و16. بينت النتائج ان معدلات التفاعل المحسوبة كانت اما قريبة من النتائج العالمية او اعلى منها بمقدار معامل 1 الى 3. أما نسب انتاج الى استهلاك نظائر الأوكسجين ^{14,15,16}O فقد بينت ان النسب تتشبع عموما عند درجات حرارة أعلى من 2 مليار كلفن، وأن النسب عموما أكثر من 1 مما يشير الى زيادة في معدل الإنتاج لهذه النظائر في النجوم العمالقة الحمر.

</div>

1. Introduction

Oxygen isotopes play a major role in the Carbon-Nitrogen-Oxygen (CNO) thermonuclear cycle which ignites in stars with masses M ≥ 1.5 to 2 Solar Mass (M$_\odot$), and

*Email: ahmed.selman@sc.uobaghdad.edu.iq

temperature threshold starting at about 1.5×10^6 K [1]. Such stars can vary in their properties to include many types, including red giants. CNO catalytic cycle, along with the proton-proton fusion (pp-chain) are the two main sources of power in most stars. CNO cycle is based on many sub-reaction processes or branches, that contain particle radiative capture, of which proton capture is dominant in light isotopes production. Many proton-radiative capture reactions are responsible for light element production in stars, such as the intense (p, α) and less competitive (p, γ) reactions.

There are many reactions in the CNO cycle where O isotopes are produced or destroyed. This creates a competition among production and destruction reactions, leading to a key factor in the overall reaction rate of the whole cycle [2]. Nuclear reaction rate represents a unique physical quantity to measure the productivity of a certain nuclear stellar reaction. Many references discuss its calculation in details [3] [4]. Furthermore, there are two famous libraries used to compare reaction rate calculations, namely BRUSLIB [5], NACRE II [6] .

In this paper, we aim to determine the compatibility between a few related reactions leading to production and destruction of 14,15,16O isotopes by means of the reaction rates of charged particle capture processes, only in the cold and hot CNO cycles. Such comparison will be taken for stellar conditions, especially Red Giant stars (RG). The reason behind choosing RG stars in relation to all O isotopes is their importance in many cosmologically-related nucleosynthesis phenomena such as H2O and dust grain production. Calculations will be performed using written MATLAB codes. Comparison data will also be used from NACRE II Library, as well as in other available sources. This research has important contribution to the evaluation of production and destruction of O isotopes in stars when comparing similar reactions with standard reaction rate libraries [5, 6].

2. Theory
2.1. Reaction Rates

In stellar environment, instead of using the cross-section for studying various reactions, it's preferred to use the reactivity, or *reaction rates* $N_A\langle\sigma v\rangle$ of the reactants. It's the product of relevant cross section times the Maxwellian-Averaged, thermally distributed velocity [7]. For the detailed theory of reaction rate calculation, we refer to the theory reviewed from the literature by Ali [3,4] and Selman [8]. $N_A\langle\sigma v\rangle$ is found basically from

$$N_A\langle\sigma v\rangle = \sqrt{\frac{8}{\pi\mu \, k^3 T^3}} \int_0^\infty S(E) \, e^{\left[-\frac{E}{kT}-2\pi\eta(E)\right]} \, dE \qquad (1)$$

where μ, η, T and k are the reduced mass, Sommerfeld parameter, temperature, and Boltzmann constant, respectively. Eq.(1) is written in terms of the *Astrophysical Spectroscopic S-Factor*, *S(E)*, instead of the cross section since the latter strongly depends on the reaction energy for most reactions. *S*-factor is given for various reactions, however, at effective stellar temperatures, it's more practical to introduce the *Effective S-Factor, S$_{eff}$* [7] into Eq.(1)

$$S_{\text{eff}} = S\left[1 + \frac{5}{12\tau} + \frac{\dot{S}}{S}\left(E_0 + \frac{35}{36}kT\right) + \frac{\ddot{S}}{2S}\left(E_0^2 + \frac{89}{36}E_0 kT\right)\right] (\text{MeV.b}) \qquad (2)$$

where τ is a dimensionless correction parameter given as $\tau = \frac{3E_0}{2kT} = 4.248(Z_1^2 Z_2^2 \mu/T_9)^{1/3}$. The final form of the non-resonant reaction rate is [8]

$$N_A\langle\sigma v\rangle = \frac{4.34 \times 10^8}{\mu \, Z_1 Z_2} S_{\text{eff}} \, \tau^2 e^{-\tau} \qquad (3)$$

In Eq. (2), τ is a numeric factor that relates to atomic numbers of target and projectile [4], and the values of the *S*-factor are taken as derivatives with respect to time. Z_1 and Z_2 are the atomic number of the projectile, and target partiles, respectively. Few other modifications could be considered when substituting Eq. (2) into Eq. (1) such as screening effects and non-symmetry of the Gamow window [3,8], but these modifications shall be ignored in this research.

2.2 Charged-Particles Capture
Thermonuclear reactions are known to produce various isotopes to the iron threshold. Above that, particle radiative capture is thought to be responsible of producing heavier elements [3]. However, even in light mass range, particle capture can significantly contribute in the production of many isotopes, some of which re-enter thermonuclear reactions again. Particle capture can occur via charged (protons, alphas, ... etc.) and/or uncharged projectiles (neutrons mainly); where at low energies, the former considerably suffers from the Coulomb barrier and the latter from resonances. In the present work we shall focus on charged particle capture processes participating in various reactions where O isotopes are involved in the exit channel.

Previous studies in this course showed few discrepancies in relation to evaluated reaction rates. Charged particles reactions at stellar energies $E < 350$ keV can undergo through few reaction channels according to their incident energy and target nucleus structure, those can be classified into three major regions: non-resonance, narrow, and broad resonances [7]. For non-resonance and broad resonance regions, Eq. (1) can be numerically integrated to find the reaction rates. Indeed, such calculations are made and found in many nuclear libraries, such as NACRE II [6]. At narrow resonances, the calculation becomes difficult since many peaks will interfere due to the minor but many contributions of Coulomb energies, thus the total estimation of theoretical values deviates from experimental ones [9], [10]. Instead, in such regions, other precise methods are followed, such as Hauser-Feshbach model [11] or the recent modified potential cluster model [1]. All such models are tested against experimentally established reaction rates, and such comparisons with experimental data were sought since the famous beginning of theoretical calculation by Fowler et al. [12].
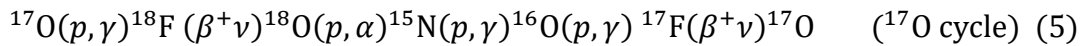
2.3. The Role of O Isotopes in Red Giant Stars
Considering the total reaction rate for O isotopes' reactions can indicate how the overall strength of the CNO cycle can be, thus determining the total energy production of a star – hence most of its properties such as luminosity, composition and life. Almost all oxygen isotopes ^{14,15,16,17,18}O undergo various capture and decay reactions in CNO cycle [2, 10-12]. The most effective sub-cycles are ^{16,17,18}O. The isotope ^{15}O also has significance in CNO cycles since it provides a branching point between various reactions, while ^{14}O isotope is the less effective among O isotopes– see below.
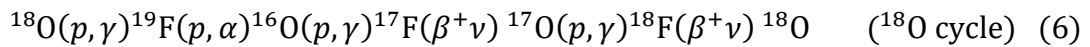
2.4. Cycles of ^{16,17,18}O Isotopes
They are part of the main CNO cycle that lie within hot and cold CNO branches. These cycles were first proposed [9,12,13] to explain how different isotopes are produced during thermonuclear reactions and highly depend on N and O target nuclei, hence they were first labeled the NO cycle. Below a list of ^{16,17}O isotopes in NO cycles initially proposed [13]:

$$^{16}\text{O}(p,\gamma)^{17}\text{F}\,(\beta^+\nu)^{17}\text{O}(p,\alpha)^{14}\text{N}(p,\gamma)^{15}\text{O}\,(\beta^+\nu)^{15}\text{N}(p,\gamma)^{16}\text{O} \qquad (^{16}\text{O cycle}) \quad (4)$$

$$^{17}O(p,\gamma)^{18}F\,(\beta^+v)^{18}O(p,\alpha)^{15}N(p,\gamma)^{16}O(p,\gamma)\,^{17}F(\beta^+v)^{17}O \qquad (^{17}O\ \text{cycle}) \quad (5)$$

A third possibility is the ^{18}O cycle:

$$^{18}O(p,\gamma)^{19}F(p,\alpha)^{16}O(p,\gamma)^{17}F(\beta^+v)\,^{17}O(p,\gamma)^{18}F(\beta^+v)\,^{18}O \qquad (^{18}O\ \text{cycle}) \quad (6)$$

Now it is well known that such cycles are part of a greater scheme in CNO process. There are one or more paths for each isotope as shown below in Figure (1) for cold CNO, and Figure (3) for hot CNO cycles. In all possible cycles, when alpha emission from ^{16}O isotope is faster than the particle capture process, the total reaction will suffer from low reactivity. In such case the less abundant ^{16}O isotope will scatter over the whole CNO cycle. ^{16}O isotope also has another key role because the reaction $^{15}N(p,\gamma)^{16}O$ is the main branching point between cold and hot CNO cycles [14].
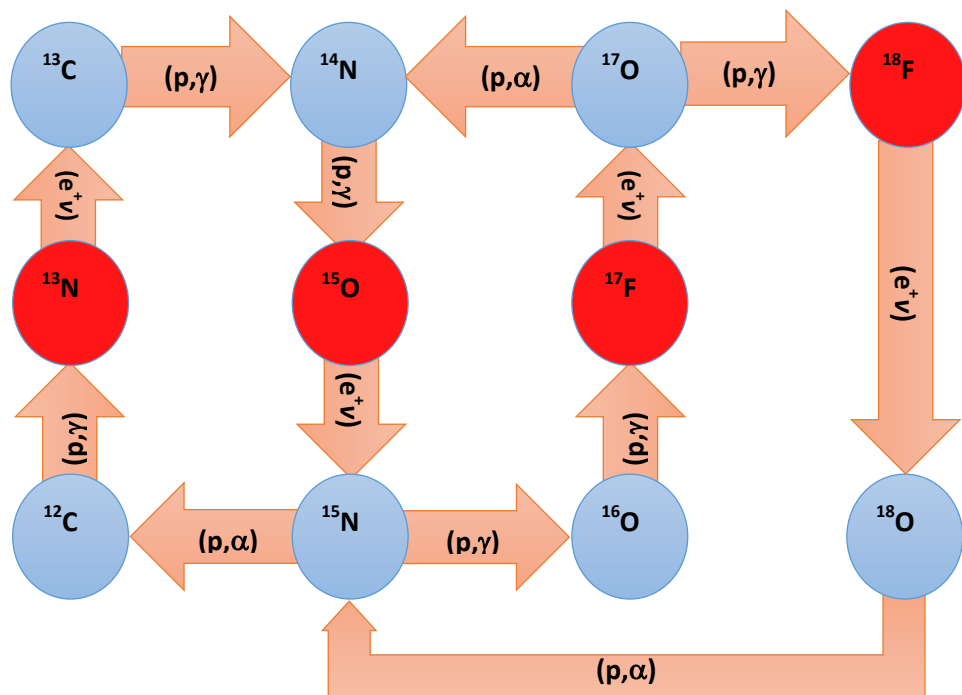

Figure 1: Cold CNO cycle, reproduced from [13].

2.5. Importance of ^{14}O Isotope

Although it is rare and has less effect than main cycles, ^{14}O isotope is thought to produce mainly in hot CNO cycle from carbon burning in the stellar core at temperature around 2.0×10^8 K from the reaction $^{13}N(p,\gamma)^{14}O$. The product is unstable against beta-decay with half-life 70.2 s [15] resulting in ^{14}N isotope. However, when ^{14}O abundancy increases and temperature rises to more than 3.8×10^8 K, other reactions will start that add new isotopes to stellar environment, such as ^{17}F isotope from $^{14}O(\alpha,p)^{17}F$ [13]. It is known that F isotopes are the rarest in the universe [8]; therefore, ^{14}O isotope has a very unique part in chemical nucleosynthesis process in the universe.

3. Samples, Calculations, Results and Discussions
3.1. Samples and Input

Next, we shall consider the most important reactions mainly responsible of producing and destroying of 14,15,16O isotopes. From Eq.s (4,5,6) and Figures (1,2), we can see there are

many reactions in CNO cycles where O isotopes are involved. From these, we select the following reactions for their significance -also see Table (1) below:

1. Producing reactions: $(\_^{19})F\ (p,\alpha)^{16}O$, $(\_^{15})N\ (p,\gamma)^{16}O$, $(\_^{14})N\ (p,\gamma)^{15}O$,$(\_^{18})F\ (p,\alpha)^{15}O$, and $(\_^{13})N\ (p,\gamma)^{14}O$.

2. Destroying reactions: $(\_^{16})O\ (p,\gamma)^{17}F$, and $(\_^{15})O\ (\alpha,\gamma)^{19}Ne$.

The reaction $(\_^{15})O\ (\alpha,\gamma)^{19}Ne$, although included in Figure (2), but it's thought to occur in explosive conditions such as X-ray bursts and supernovae [18]. Other reactions will be left for further investigation, including $(\_^{18})O\ (p,\alpha)^{15}N$,$(\_^{(}18))O\ (\alpha,\gamma)^{22}Ne$ (negligible [13]), $(\_^{17})O\ (p,\alpha)^{14}N$,$(\_^{12})C\ (\alpha,\gamma)^{16}O$, $(\_^{13})C\ (\alpha,n)^{16}O$, $(\_^{14})N\ (\alpha,\gamma)^{18}F(\beta^{+}+\nu)^{18}O$, and $(\_^{16})O\ (\alpha,\gamma)^{20}Ne$.

3.2. Reaction Rates Calculation

A few MATLAB codes have been written to calculate reaction rates in this research without resonance using Eqs.(1, 2 and 3) and data from Table (1). The main code first finds the effective *S*-factor and then performs the detailed calculations. It should be noted that $\dot{S}$ and $\ddot{S}$ are usually much lower than $S(0)$, hence they are usually ignored in such calculations [16]. Physical input parameters were taken as found in the literature [3,5,6,8,16] for each sample reaction. The maximum temperature was fixed at $T=10$ GK (or $T_9=10$) for all reactions. Some of the calculated reaction rates values were compared with those available in NACRE II [6]. Otherwise, it was mentioned the type of confidence made for accepting the results. During each calculation, the resultant values of effective *S*-factor and τ were plotted. An example is shown in Figure (3) for the reaction $^{14}N(p,\gamma)^{15}O$. Below are the results of chosen reactions in the present research.

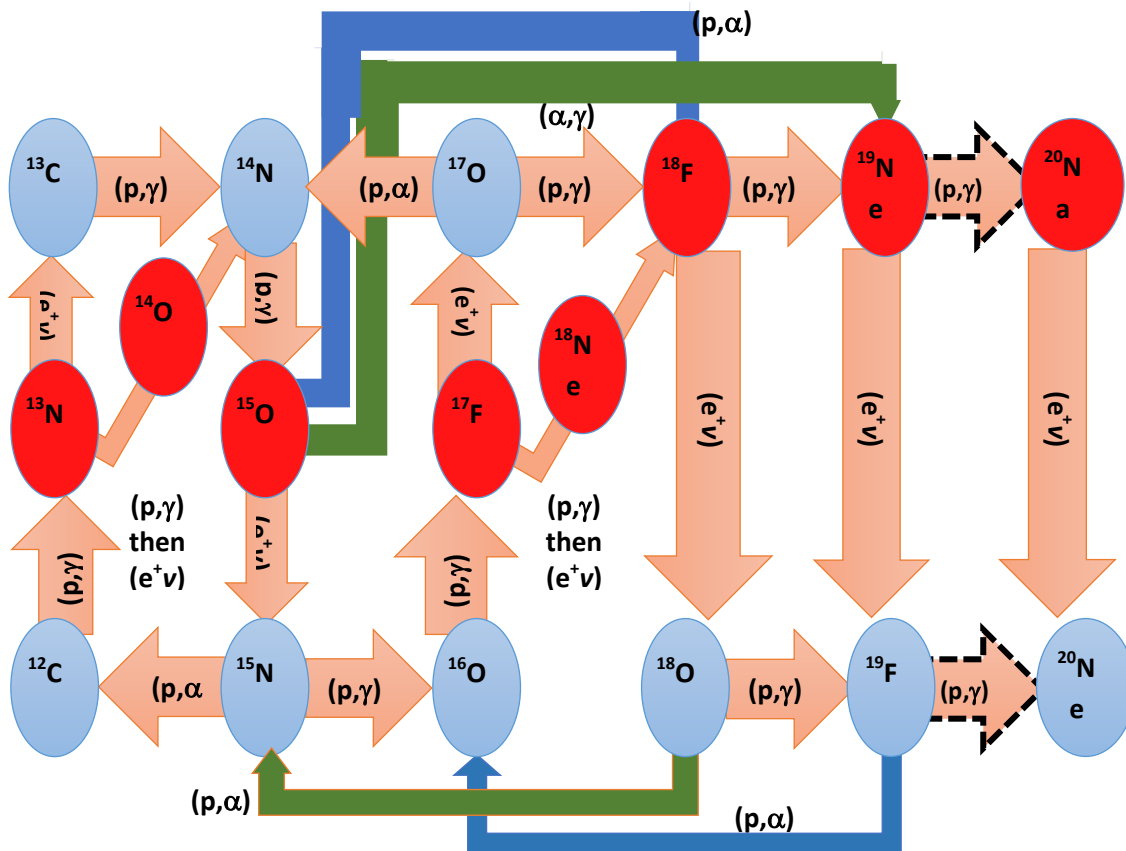**Figure 2**: Hot CNO cycle, reproduced from [13]. Note how 14O and 18N go through (p, □) reaction and then suffer from β+ decay to create sub-branching points in the cycle. Also note the production of Na-Ne isotopes occur outside the CNO cycle.

Table 1: Calculated Q-values of ^{14,15,16}O isotopes in the hot and cold CNO cycles, at E_{lab}=0.3 MeV selected from [17]. Also $S(0)$ values from literature are listed.

eaction	Q-value (MeV)	S(0) keV.b	Reference	Remarks
$^{19}\mathbf{F}(p,\alpha)^{16}\mathbf{O}$	8.11	2.40×10^4	[10] and [16]	Production, hot CNO only.
$^{15}\mathbf{N}(p,\gamma)^{16}\mathbf{O}$	12.12	36.0 39.6 64.0	[2] [14] [18]	Production, hot CNO only. This is the main branching point between hot and cold CNO.
$^{14}\mathbf{N}(p,\gamma)^{15}\mathbf{O}$	7.29	3.20 1.77	[18] [19]	Production, hot and cold CNO. This is the slowest in cold CNO.
$^{18}\mathbf{F}(p,\alpha)^{15}\mathbf{O}$	2.88	2.40	[16]	Production, hot CNO only.
$^{13}\mathbf{N}(p,\gamma)^{14}\mathbf{O}$	4.62	≈ 5	[1]	Production, hot CNO only.
$^{16}\mathbf{O}(p,\gamma)^{17}\mathbf{F}$	0.60	4.0 9.30	[10] [18]	Destruction, hot and cold CNO. This reaction is competing with the branch $^{17}\text{F}(p,\gamma)^{18}\text{N}(\beta^+\nu)^{18}\text{F}$.
$^{15}\mathbf{O}(\alpha,\gamma)^{19}\mathbf{Ne}$	3.52	2×10^4	[10] and [16]	Destruction, hot CNO only. Rapid *rp* process occur in cycles during explosive conditions [16].

3.2.1. Reaction $^{19}F(p,\alpha)^{16}O$

Figure (4) shows the reaction rates calculation in the present work for this reaction. For comparison, theoretical data for the reaction is found in Angulo et al. [18] and Indelicato et al. [20] in formulated relation and it was re-calculated and used for comparison with the present results. Present values are generally lower than both references. However, it was mentioned [18] that there was some debate about the values of reaction rates for this reaction due to the variance in thermal energy, thus few factorization techniques had been adopted. In this research there has been no factorizing for the calculated values. Also there was uncertainty in determining the value of S(0) due to scattered resonance at low energies (less than 160 keV) that made large difference between reactions from Angulo et al. [18] and Indelicato et al. [20] to reach to a factor of about 5. Data from Angulo et al. were calculated from the formula found in [18] and those of Indelicato et al. from Eq.(14) in [20].

For this reaction, a power curve fitting was made for the present results. Few relations have been tried, and we think the best result was the power relation for this reaction as well as the rest. The present curve fitting gave the following formula

$$N\_A \langle \sigma v \rangle\_ = 8.555 \times [\![10]\!]^5 \, T\_9^{2.384} - 2.856 \times [\![10]\!]^4 \qquad (7)$$

The goodness of this fit as all the others was R>98%, which gave a good confidence. Another reason that we chose to make the present curve fitting is for the sake of further comparison between the results of production rates and destruction calculations which will be given in Section 3.3. The obvious benefit of Eq. (7) is to make a comparison with other calculations much easier than to calculate Eq.(1 through 4). The better the goodness of this fit, the more reliable it would be.
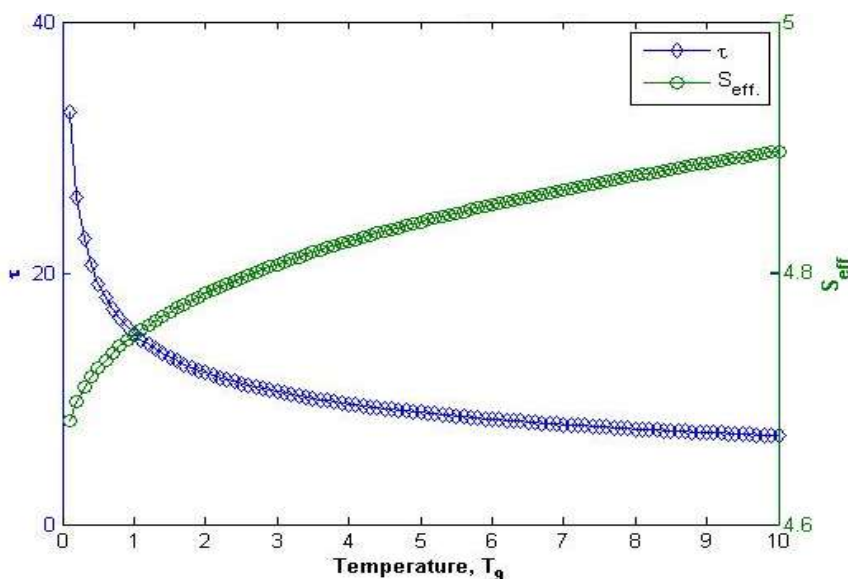
Figure 3: An example of the present calculations for the effective *S*-factor and τ values for the reaction $^{14}\mathrm{N}(p,\gamma)^{15}\mathrm{O}$.

3.2.2. Reaction $^{16}O(p,\gamma)^{17}F$

In the Figure (5), the present calculation results are shown, and a comparison with the theoretical data from Angulo et al. [18]. Data from [18] was re-calculated and used for comparison with the present results. Two formulas were listed by Angulo et al. as shown in the figure, one for the ground state, and the other for the first excited state. This reaction has resonances at high energies, 2.53 MeV and 3.55 MeV, thus at lower energies data were consistent with the present calculations for the ground state (green dotted line in the figure). The value of S(0) was taken as 4.00 [10]. For this reaction, the curve fitting gave the following formula

$$N_A\langle\sigma v\rangle = 2.702 \times 10^5 T_9^{2.158} - 6.472 \times 10^5 \qquad (8)$$

3.2.3. Reaction $^{18}F(p,\alpha)^{15}O$

From the Figure (6), the comparison with other data is shown. The data found in [16] was also in a formulated relation and it was re-calculated in this research and used for comparison with the present results. Generally, the present results were lower than Illidis et al. [16] at low energies and higher at higher energies, but statistics showed that the difference is ~ 10%. Curve fitting of reaction rates in this case gives:

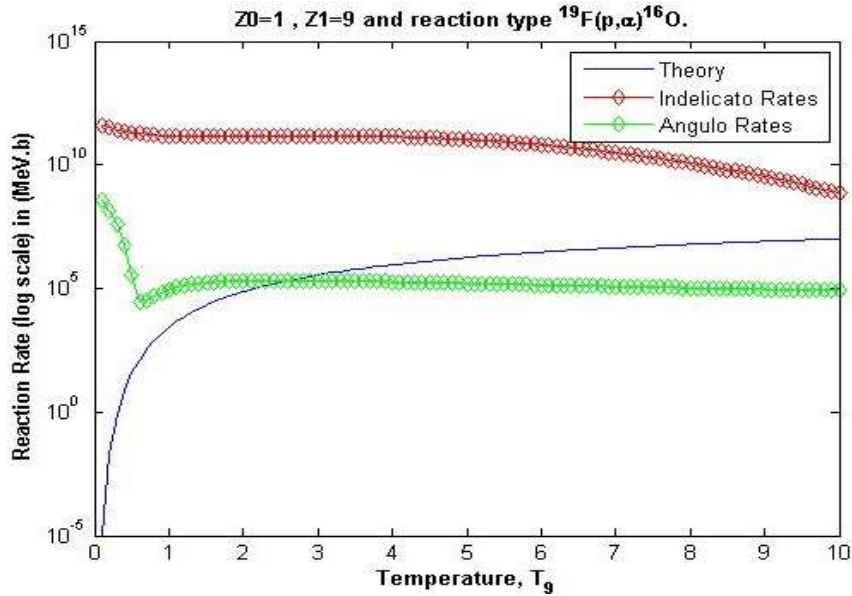$$N_A\langle\sigma v\rangle = 1.491 \times 10^5 T_9^{2.381} - 4.56 \times 10^5 \qquad (9)$$

Figure 4: Reaction rate values vs. temperature for the reaction $^{19}F(p,\alpha)^{16}O$ (solid blue line) compared with those of Indelicato et al. [20] (red dotted line) and Angulo et al. [18] (green dotted line).
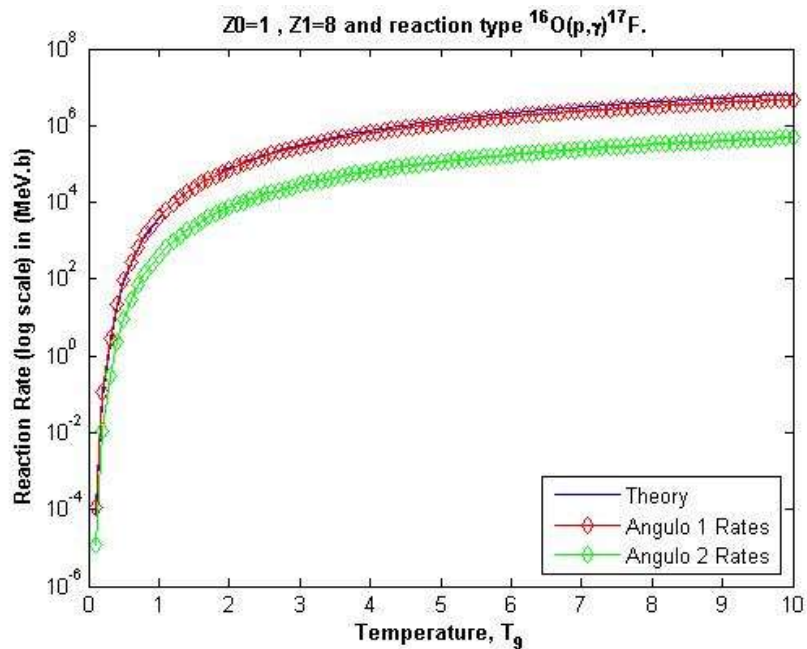

Figure 5: Reaction rate values vs. temperature for the reaction $^{16}O(p,\gamma)^{17}F$ (solid blue line) compared with those of Angulo et al. [18] (red and green dotted lines)

3.2.4. Reaction $^{15}N(p,\gamma)^{16}O$

Figure (7) shows the reaction rates calculation in the present work for this reaction. Experimental data for the reaction were found in NACRE II library and it was used for comparison with the present results. This reaction has resonance to about energy 2.3 MeV above, and it is usually assumed that the S-factor is constant [18]. The adopted value of the S-factor in the present calculation was as in ref. [3], S(0)= 36 keV. The differences with present results were of about a factor 2 .

In the cold CNO cycle, this reaction has two distinctive features [2]: (1) will cause the breakout from cold cycle, and (2) it is the main energy supply from this cycle. For this reaction the best result for curve fitting is

$$N_A\langle\sigma v\rangle = 2.188 \times 10^3 T_9^{1.929} - 3.811 \times 10^3 \tag{10}$$

3.2.5. Reaction $^{13}N(p,\gamma)^{14}O$

Figure (8) gives the calculated reaction rates in the present work and their comparison with experimental data as found in NACRE II library [6]. A very good match is seen at $T_9>0.2$ in this example. In this reaction, power curve fitting formula is as follows:

$$N_A\langle\sigma v\rangle = 2.287 \times 10^5 T_9^{1.921} - 3.492 \times 10^5 \tag{11}$$
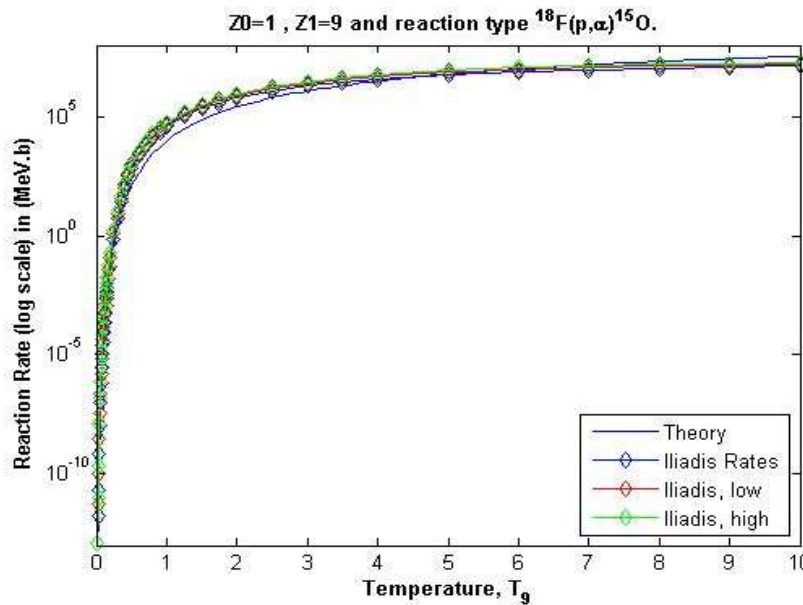

Figure 6: Reaction rate values vs. temperature for the reaction $^{18}F(p,\alpha)^{15}O$ (solid blue line) compared with those of Illiadis et al. [16] (dotted lines).
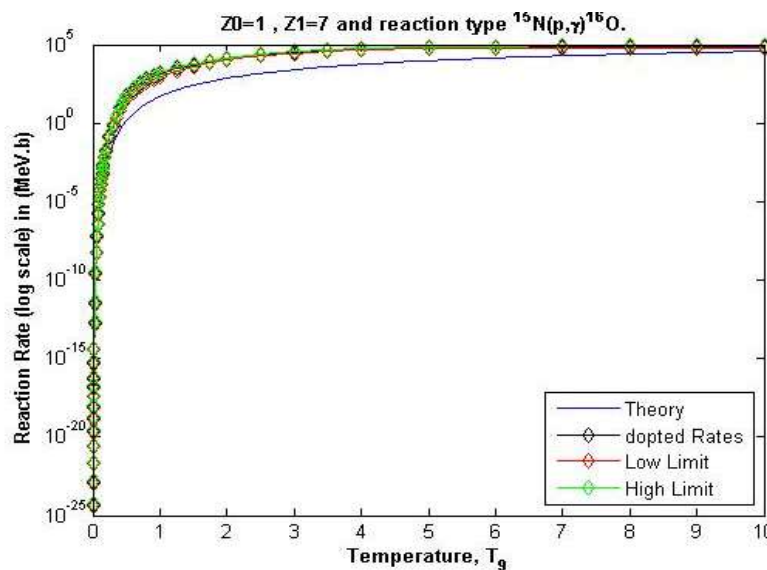

Figure 7: Reaction rate values vs. temperature for the reaction $^{15}N(p,\gamma)^{16}O$ (solid blue line) compared with those of NACREII [6] (dotted lines).

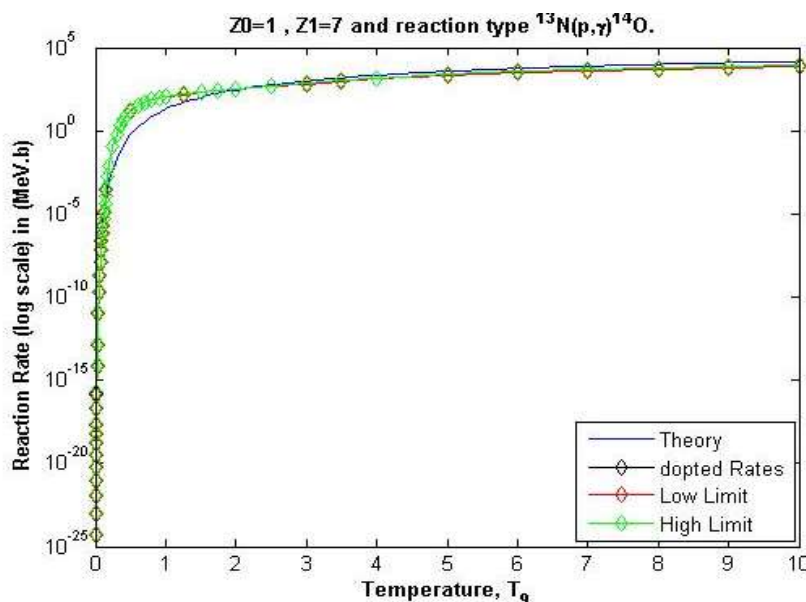**Figure 8**: Reaction rate values vs. temperature for the reaction $^{13}N(p,\gamma)^{14}O$ (solid blue line) compared with those of NACREII [6] (dotted lines).

3.2.6. Reaction $^{14}N(p,\gamma)^{15}O$

I n Figure (9) the reaction rates are shown and compared with data from NACRE II library [6], and it was used for comparison with the present results. At 0.1<T9<0.7 there was a difference of about a factor of 2. The best result of the power relation was as follows:

$$N_A\langle\sigma v\rangle = 5.36 \times 10^3 T_9^{1.925} + 9.29 \times 10^2 \tag{12}$$

3.2.6. Reaction $^{15}O(\alpha,\gamma)^{19}Ne$

Finally, $^{15}O(\alpha,\gamma)^{19}Ne$ rates and their comparison with JINA Reaclib [21] are shown in Figure (10). Generally, our present calculations deviate from those of Reaclib at T_9>5 K, and this is probably due to the uncertainty in the values of $S(0)$ for this reaction. Curve fitting for the resultant rates is found for present results as:

$$N_A\langle\sigma v\rangle = 4.882 T_9^{2.155} - 11.49 \tag{13}$$

3.3. Production and Destruction of $^{15,16}O$ Isotopes

Ratios between production to destruction rates for 15,16O isotopes in the CNO cycle were calculated in this research and the results are given in Figure (11). Cold CNO cycle does not include 14O, and the hot CNO actually has this isotope produced and destroyed within the first cycle. Production of this isotope was calculated presently, however; the destruction of 14O is via beta decay, (e+v), which was not included in the present calculation. Beta decay reaction, (e+v), was not included here because its reaction takes longer time than the particle capture in the s-process. If these reactions were faster than the neutron capture, the s-process cycle (Figure 1 and 2) will no longer be applied, and the calculations should be made for the rapid capture (r-process) which is of very small probability in CNO cycles. Therefore, in Section 3.1. (Samples and Input), no beta decay reactions were selected for any of the isotopes 14,15,16O.

Figure (11) was plotted using the curve fitting equations, Eq.s (8-10, 11-13), then the ratios were directly found at each temperature T9 then plotted. From Figure (11) a few central remarks can be pointed out. First, both ratios reach a saturation level atT_9≥2 K. 15O ratio was also constant to about T_9≤1.4 K. At the region between these two degrees, a substantial

change is noticed in both ratios. These changes clearly indicate an excess of production of both isotopes in these cycles. However, due to the many approximations used in the present calculation; we think that the results shown in Figure (11) overestimate the real conditions at least by a factor of 1. The most important factor that should be kept in mind here is the many possible resonance peaks occurring at low temperatures during many of the selected reactions which could add important changes to the final results. Therefore, it is recommended to include these reactions in more detailed calculations. The very special structure of 16O nucleus (having closed shells for protons and neutrons) and the large value of S(0) reported for $(\_{}^{19})F\ (p,\alpha)^{16}O$ reaction can add a certain amount of error to the results. Yet, the present calculations can give a rough estimate of the productivity of 15,16O isotopes in RG stars during CNO both hot and cold cycles.
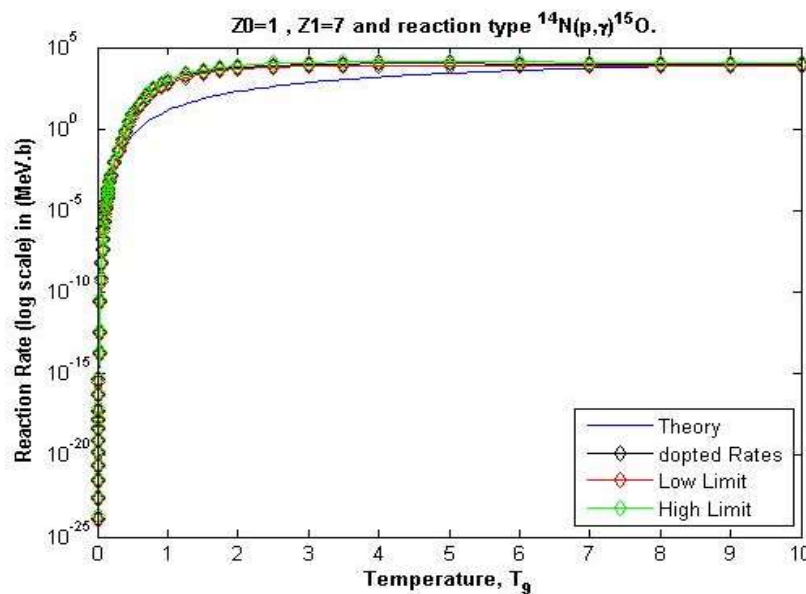

Figure 9: Reaction rate values vs. temperature for the reaction $^{14}N(p,\gamma)^{15}O$ (solid blue line) compared with those of NACREII [6] (dotted lines).

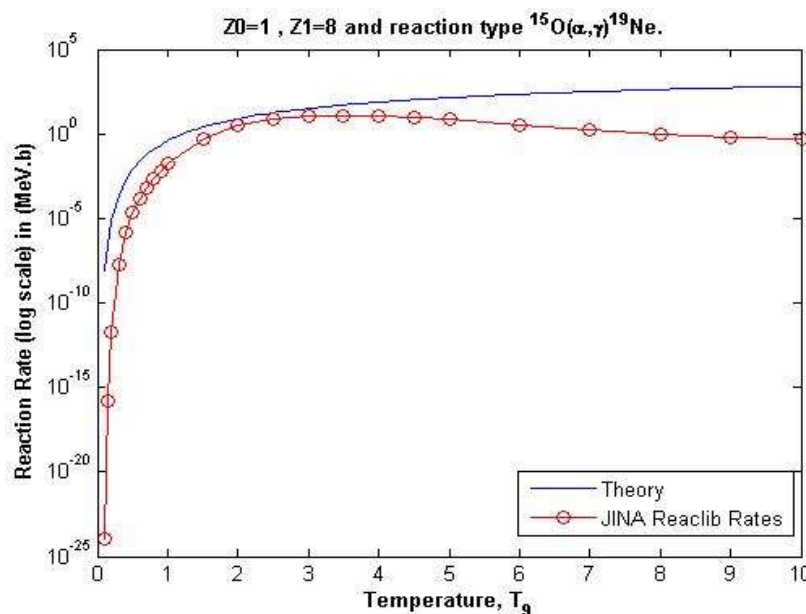**Figure 10:** Reaction rate values vs. temperature for the reaction $^{15}O(\alpha,\gamma)^{19}Ne$ (solid blue line) compared with those of Reaclib [21] (dotted red line).
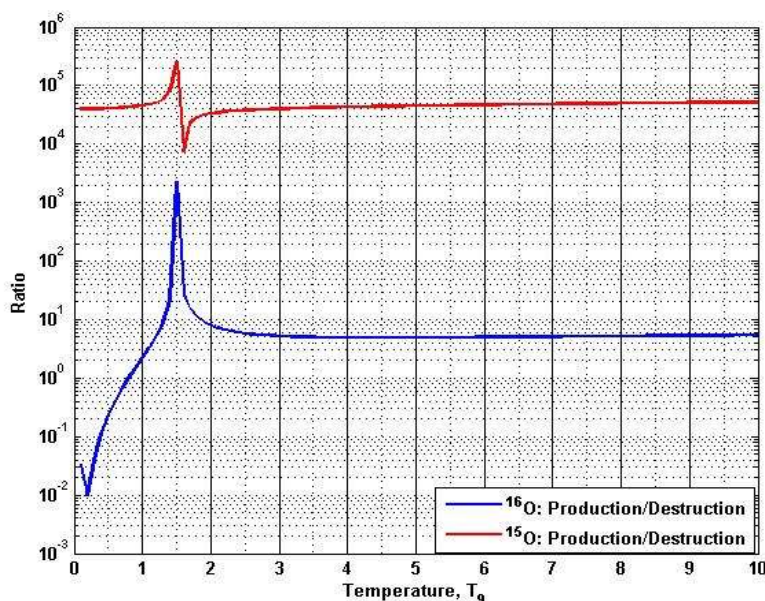
Figure 11: A comparison between present reaction rates for production to destruction ratios for ^{15,16}O isotopes.

4. Conclusions

Some of the O isotopes reactions occurring during hot and cold CNO cycles have been studied by means of reaction rates. It's seen that the ratios of production of both 15,16O isotopes tend to be quite larger than 1, indicating an extra production for both of these isotopes. The present results overestimate real ones due to a few parameters, the most important is being the possible resonances at lower temperatures for most of the reactions involved in the present calculations yet omitted here. It was recommended to include resonance reactions at lower temperatures and take special care of calculating the value of S(0) for 16O production reactions.

Reference

[1] S. B. Dubovichenko, R. Ya. Kezerashvili, N. A. Burkova, A. V. Dzhazairov-Kakhramanov, and B. Beisenov, "Reanalysis of the 13N(p,γ)14O Reaction and its Role in the Stellar CNO Cycle," *Physical Review C,* vol. 102, no. 4, p. 045805, 2020.

[2] G. Stasińska, Oxygen in the Universe, Chapter 3, EDP Sciences, 2012, pp. 187-253.

[3] L. T. Ali, *Ph.D. Thesis: Calculation of Stellar Nuclear Reaction Rate for Low and Intermediate Mass Nuclei,* Baghdad-Iraq, 2021.

[4] L. T. Ali and A. A. Selman, "Non-Resonant Reaction Rates of 13C(α,n)16O and 22Ne(α,n)25Mg Reactions in AGB Stars," *Iraqi Journal of Science,* vol. 62, no. 5, pp. 1734-1744, 2021.

[5] "BRUSLIB Library," [Online]. Available: http://www.astro.ulb.ac.be/bruslib/index.html. [Accessed 20 4 2022].

[6] "NACRE II Library," [Online]. Available: http://www.astro.ulb.ac.be/nacreii/index.html. [Accessed 16 April 2022].

[7] C. Iliadis, Nuclear Physics of Stars, 2 ed., Wiley-VCH Verlag GmbH & Co., 2015.

[8] A. A. Selman, "Impact of Neutron Sources of Stellar Reactions on Fluorine Abundancies," *Accepted for publication at the Iraqi J. Science on Feb. 2023.,* 2023.

[9] C. Sivaram, V. de Sabbata, and Y. Yellappa, "Production of Rare Isotopes Such as Li-7, B-11 and F-19 by High Energy Neutrinos from Supernovae," in *Proceedings of the 21st International Cosmic Ray Conference. Volume 3 (OG Sessions)*, 1991.

[10] C. Iliadis, R. Longland, A. E. Champagne, A. Coc, and R. Fitzgerald, "Charged-Particle Thermonuclear Reaction Rates II. Tables and Graphs of Reaction Rates and Probability Density Functions," *Nuclear Physics A,* vol. 841, no. 1-4, pp. 31-250, 2010.

[11] W. A. Fowler, G. R. Caughlan and B. A. Zimmerman, "Thermonuclear Reaction Rates," *Annual Review of Astronomy and Astrophysics,* vol. 5, pp. 525-570, 1967.

[12] W. A. Fowler, G. R. Caughlan, and B. A. Zimmerman, "Thermonuclear Reaction Rates, II," *Annual review of Astronomy and Astrophysics,* vol. 13, no. 1, pp. 69-112, 1975.

[13] M. Weischer, F. Kaeppeler, and K. Langanke, "Critical Reactions in Contemporary Nuclear Astrophysics," *Annual Review of Astronomy and Astrophysics,* vol. 50, pp. 165-210, 2012.

[14] P. J. LeBlanc et al., "Constraining the S Factor of 15N(p,γ)16O at Astrophysical Energies," *Physical Review C,* vol. 84, p. 019902, 2011.

[15] M. Wiescher, G. P. A. Berg, M. Couder, J. L. Fisker, Y. Fujita, J. Görres, M. N. Harakeh, K. Hatanaka, A. Matic, W. Tan, and A. M. van den Berg, "Astrophysical Nuclear Reactions and the Break-out from the Hot CNO Cycles," *Progress in Particle and Nuclear Physics,* vol. 59, no. 1, pp. 51-65, 2007.

[16] C. Iliadis, R. Longland, A. E. Champagne, and A. Coc, "Charged-Particle Thermonuclear Reaction Rates: III. Nuclear Physics Input," *Nuclear Physics A,* vol. 841, no. 1-4, pp. 251-322, 2010.

[17] "National Nuclear Data Center (NNDC), Q-value Calculator (QCalc)," [Online]. Available: https://www.nndc.bnl.gov/qcalc/qcalcr.jsp. [Accessed 16 4 2022].

[18] C. Anguloa, M. Arnould, M. Rayet, P. Descouvemont, D. Baye, C. Leclercq-Willain, A. Coc, S. Barhoumi, P. Aguer, C. Rolfs, R. Kunz, J. W. Hammer, A. Mayer, T. Paradellis, S. Kossionides, C. Chronidou, K. Spyrou, S. Degl'Innocenti, G. Fiorentini, B. Ricci, "A Compilation of Charged-Particle Induced Thermonuclear Reaction Rates," *Nuclear Physics A,* vol. 656, no. 1, pp. 3-183, 1999.

[19] C. Angulo, and P. Descouvemont, "The 14N(p,gmma)15O Low-Energy S-Factor," *Nuclear Physics A,* vol. 690, no. 4, pp. 755-768, 2001.

[20] I. Indelicato, M. La Cognata, C. Spitaleri, V. Burjan, S. Cherubini, M. Gulino, S. Hayakawa, Z. Hons, V. Kroha, L. Lamia, M. Mazzocco, J. Mrazek, R. G. Pizzone, S. Romano, E. Strano, D. Torresi, and A. Tumino, "New Improved Indirect Measurement of the 19F(p, α)16O Reaction at Energies of Astrophysical Relevance," *The Astrophysical Journal,* vol. 845, no. 1, p. 19, 2017.

[21] "JINA Reaclib Database," . [Online]. Available: https://reaclib.jinaweb.org/results.php. [Accessed 10 4 2022].